optimization procedure. The optimization is carried out by simple comparisons, enabling the procedure to be used easily on a personal computer. Even if a rather coarse grid and as few as three allowable values for control are used, convergence is rapid and the results are reliable.

References

[1] R. E. Bellman and S. E. Dreyfus, *Applied Dynamic Programming.* Princeton, NJ: Princeton Univ. Press, 1962.

[2] L. Lapidus and R. Luus, *Optimal Control of Engineering Processes.* Waltham, MA: Blaisdell, 1967.

[3] R. Luus, "Optimal control by dynamic programming using accessible grid points and region contraction," *Hungarian J. Industrial Chem.*, vol. 17, pp. 523–543, Dec. 1989.

[4] ——, "Optimal control by dynamic programming using systematic reduction in grid size," *Int. J. Contr.*, vol. 51, pp. 995–1013, May 1990.

[5] ——, "Application of dynamic programming to singular optimal control problems," in *Proc. 1990 Amer. Contr. Conf.*, May 1990, pp. 2932–2937.

[6] ——, "Application of dynamic programming to high-dimensional nonlinear optimal control problems," *Int. J. Contr.*, vol. 52, pp. 239–250, July 1990.

[7] R. Luus and D. E. Cormack, "Multiplicity of solutions resulting from the use of variational methods in optimal control problems," *Can. J. Chem. Eng.*, vol. 50, pp. 309–311, Apr. 1972.

[8] R. Luus, and M. Galli, "Multiplicity of solutions in using dynamic programming for optimal control," *Hungarian J. Industrial Chem.*, vol. 19, pp. 55–62, Mar. 1991.

[9] S. Park, and W. F. Ramirez, "Optimal production of secreted protein in fed-batch reactors," *AIChE J.*, vol. 34, pp. 1550–1558, Sept. 1988.

VSC Coordinated Control of Two Manipulator Arms in the Presence of Environmental Constraints

B. Yao, W. B. Gao, S. P. Chan, and M. Cheng

Abstract—**A variable structure control (VSC) method is developed for motion, internal force, and constrained force control of two manipulators grasping a common constrained object. Based on a transformed dynamic equation of the entire system in the joint space, motion and force control are designed together via a VSC method with robustness to parametric uncertainties and external disturbances. The proposed VSC controller guarantees the system with prescribed qualities in the sliding mode and during the reaching transient. Simulation results illustrate the proposed method.**

I. Introduction

Coordinated control of two manipulator arms has received increasing attention in recent years because of the potential applications in assembly as well as the handling of large and heavy objects which are beyond the load capacity of a single arm.

Manuscript received September 6, 1990; revised July 26, 1991. Paper recommended by Past Associate Editor, M. Spong.

B. Yao and S. P. Chan are with the School of Electrical and Electronic Engineering, Nanyang Technological University, Nanyang Avenue, Singapore 2263.

W. B. Gao and M. Cheng are with The Seventh Research Division, Beijing University of Aeronautics and Astronautics, Beijing 10083, People's Republic of China.

IEEE Log Number 9203067.

When two robots grasp a common object, they form a closed kinematic chain mechanism. This will impose a set of homogeneous constraints on the positions of the robots. As a result, degrees of freedom (DOF) of the whole system decrease, and internal forces are generated and needed to be controlled [1]–[6].

When the grasped object comes in contact with rigid surfaces, kinematic constraints are imposed on the motion of the object and contact forces are generated. It is necessary to control both the motion of the object on the constraint surfaces and the generalized constrained force. This problem has been extensively studied in recent years for a single arm [11]–[13] which is referred to nonlinear singular system [11].

The problem of constrained object grasped by multiple robots has been discussed in [7]–[10]. Nonlinear state feedback is used to linearize and decouple the robot system with respect to the object motion, internal force, and constrained force by Yun [7] and Yoshikawa and Zheng [8]. The methods are based on the exact model of the system. To deal with the uncertainties in the dynamic modeling of the system, Hu and Goldenberg [10] derived an adaptive law from Popov hyperstability theory. The controller needs the measurements of acceleration and force derivative. A VSC method [9] is developed for motion and constrained force control of the object, in which the internal force control is not considered.

In this note, we study the robust motion, internal force, and external contact force control problem of two manipulators grasping a common object which is constrained by the environment in the presence of parametric uncertainties and external disturbances both in the robot and in the object. The dynamic equations of the robots combining with the dynamic and kinematic constraints imposed on the manipulators and the object are reformulated in the joint space. Based on a transformed dynamic equation of the robotic system, motion and force control are designed together via a VSC method. The proposed VSC controller can guarantee the system with prescribed qualities both in the sliding mode and during the reaching transient. Simulation results of two three-DOF robots grasping a common object moving on a circular surface are given to illustrate the proposed method.

II. Dynamic Equation of Robotic System and Problem Formulation

Consider two n_i-joint serial link manipulators handling a rigid object in an n_0 dimensional workspace where $n_0 \le n_i$. It is assumed that both robot end-effectors grasp the object firmly at two specified points. Hence, a closed-loop kinematic chain mechanism is formed. Kinematic constraints are imposed on the relative motion between the end-effectors throughout the entire period during which the task is performed.

Let OXYZ, $O_iX_iY_iZ_i$ (see Figs. 1 and 2) be the Cartesian reference frame and the base reference frame of the ith robot, respectively. oxyz is the object frame fixed relative to the object and $o_{ei}x_{ei}y_{ei}z_{ei}$ is the end-effector frame of the ith robot located at the grasped point. The dynamic equation of the ith robot can be written as

$$M_i(q_i)\ddot{q}_i + C_i(q_i, \dot{q}_i)\dot{q}_i + G_i(q_i) + J_i^T(q_i)F_{ei} + \tilde{f}_i(t) = \tau, \qquad i = 1,2 \quad (1)$$

where q_i is the $n_i \times 1$ joint displacement vector, τ_i is the

0018-9286/92$03.00

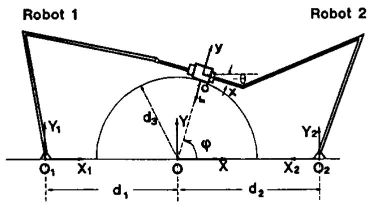

Fig. 1. Configuration of the robotic system.

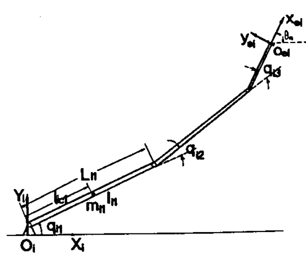

Fig. 2. Configuration of the ith robot.

applied joint torque, $M_i(q_i)$ is the inertia matrix, $C_i(q_i, \dot{q}_i)\dot{q}_i$ is the coriolis and centrifugal vector, $G_i(q_i)$ is the gravitational vector, $\tilde{f}_i(t)$ is the external disturbance, F_{ei} is the $n_0 \times 1$ vector of forces/moments on the object exerted by the ith robot at the end-effector, $J_i(q_i) = \partial x_i(q_i)/\partial q_i$ is the corresponding manipulator Jacobian matrix which is assumed to be of full rank in the work space and x_i is the $n_0 \times 1$ position and orientation vector of the end-effector frame $o_{ei}x_{ei}y_{ei}z_{ei}$ in the base reference frame $O_iX_iY_iZ_i$. The dynamic equation of the grasped object can be written as

$$M_0(p)\ddot{p} + C_0(p, \dot{p})\dot{p} + G_0(p) + \tilde{f}_0(t) = \sum_{i=1}^{2} F_i - F_c \quad (2)$$

where p is the $n_0 \times 1$ position and orientation vector of the object frame oxyz in OXYZ, $M_0(p), C_0, G_0(p), \tilde{f}_0(t)$ have the same meaning as in (1), F_c is the contact force vector on the environment exerted by the object, F_i is the equivalent force representation of F_{ei} given by

$$F_i = L_i^{-T} F_{ei} \qquad F_{ei} = L_i^T F_i \quad (3)$$

where L_i is the nonsingular transformation matrix between the object position and the ith robot end-effector position given by

$$\dot{p} = L_i(x_i)\dot{x}_i \qquad L_i(x_i) = \frac{\partial p(x_i)}{\partial x_i}. \quad (4)$$

The kinematic constraints resulted from the closed chain mechanism can be written as

$$p = p(x_i) = p(x_i(q_i)) = \Phi_i(q_i) \qquad \dot{p} = A_i(q_i)\dot{q}_i$$

$$\ddot{p} = A_i\ddot{q}_i + \dot{A}_i\dot{q}_i \quad A_i \equiv L_i(x_i(q_i))J_i(q_i) \in R^{n_0 \times n_i} \quad i = 1, 2. \quad (5)$$

Equations (1) and (2) have the following properties [13]. (For simplicity, we use q_0 for p).

Property 1: $M_i(q_i)$ is a symmetric positive definite matrix. Moreover, for any finite workspace Ω_i, there exist $k_i' > 0$ and $k_i'' > 0$ such that $k_i' I_{n_i} \le M_i(q_i) \le k_i'' I_{n_i}$ $\forall q_i \in \Omega_i$ $i = 0, 1, 2$ where I_{ni} is the $n_i \times n_i$ identity matrix.

Property 2: The matrix $N_i(q_i, \dot{q}_i) = \dot{M}_i(q_i) - 2C_i(q_i, \dot{q}_i)$ is a skew-symmetric matrix.

Property 3: A part of the dynamic structure is linear in terms of a suitably selected set of the robot (the object) parameters, i.e.,

$$M_i(q_i)\ddot{q}_{\mathrm{ieq}} + C_i(q_i, \dot{q}_i)\dot{q}_{\mathrm{ieq}} + G_i(q_i) = Y_i\left(q_i, \dot{q}_i, \dot{q}_{\mathrm{ieq}}, \ddot{q}_{\mathrm{ieq}}\right)\beta_i \qquad i = 0, 1, 2 \quad (6)$$

where Y_i is a $n_i \times k_i$ matrix and β_i is a $k_i \times 1$ vector containing the unknown manipulator (the object) parameters; $\dot{q}_{ieq}, \ddot{q}_{ieq}$ are reference velocity and acceleration, respectively.

Due to parametric uncertainties, the exact values of β_i are not known and the available values are assumed to be $\hat{\beta}_i$. The modeling errors in (1) and (2) are assumed to be bounded by

$$|\Delta\beta_i| \le \delta\beta_i \qquad \Delta\beta_i = \beta_i - \hat{\beta}_i$$
$$|\tilde{f}_i(t)| \le \delta\tilde{f}_i(t) \qquad i = 0, 1, 2 \quad (7)$$

where $|A| \le B$ is true in element, i.e., $|A_{ij}| \le B_{ij}$ and boundary values $\delta\beta$ and $\delta\tilde{f}_i(t)$ are known. (In the following, the operation of matrix is understood in the same meaning.)

When the object comes in contact with an environment which is completely rigid, the object motion is constrained on the contact surfaces. We assume that the environmental constraints can be represented by m mutually independent smooth hypersurfaces:

$$\Phi_0(p) = 0 \qquad \Phi_0(p) = [\phi_{01}(p), \cdots, \phi_{0m}(p)]^T \quad (8)$$

Neglecting friction force, the contact force F_c is given by [8], [11]–[13]

$$F_c = J_c^T(p)f_n \qquad J_c(p) = \frac{\partial \Phi_0(p)}{\partial p} \quad (9)$$

where f_n is a $m \times 1$ vector of Lagrange multipliers associated with the constraints. It is assumed that the object initially lies on the constraint manifold $\{\Phi_0(p) = 0,\ J_c(p)\dot{p} = 0\}$ and the control exercised over the object is to maintain motion of the object on it [11], [12]. In this case, it is necessary to control both the motion of the object on the constraint surfaces (8) and the generalized constrained force f_n. However, this will only determine the sum of the forces applied by the two end-effectors. Since there is a redundancy in determining the forces F_i exerted by each robot, we must also ensure the necessary coordination between them. This can be achieved by controlling the internal force in the object [1]–[6]. The internal force is defined as

$$f_{\mathrm{int}} = (1 - \alpha)F_1 - \alpha F_2 \qquad 0 \le \alpha \le 1 \quad (10)$$

where α is a constant weighting factor.

The above dynamic equations and constraints of the robotic system are derived directly from the physical laws. In the following, we will reformulate these equations and constraints to obtain an equivalent set in the joint space in terms of the joint vector $q = [q_1^T, q_2^T]^T \in R^{n1+n2}$ and the controlled force $f = [f_{int}^T, f_n^T]^T \in R^{n0+m}$ in a form which is suitable for designing control algorithms. From (2) and (10), we have

$$F_1 = \alpha(M_0\ddot{p} + C_0\dot{p} + G_0 + F_c + \tilde{f}_0) + f_{\mathrm{int}}$$
$$F_2 = (1 - \alpha)(M_0\ddot{p} + C_0\dot{p} + G_0 + F_c + \tilde{f}_0) - f_{\mathrm{int}}. \quad (11)$$

Substituting the above and (3), (5), and (9) into (1), the resulting equation can be written in a concise form

$$M(q)\ddot{q} + C(q, \dot{q})\dot{q} + G(q) + \tilde{f}(q, t) = \tau - D^T(q)f \quad (12)$$

where

$$M(q)=\begin{bmatrix} M_1(q_1)+\alpha A_1^T M_0(p)A_1 & \\ & M_2(q_2)+(1-\alpha)A_2^T M_0(p)A_2\end{bmatrix}\in R^{(n_1+n_2)\times(n_1+n_2)}$$

$$C(q,\dot q)=\begin{bmatrix} C_1(q_1,\dot q_1)+\alpha A_1^T C_0 A_1+\alpha A_1^T M_0 \dot A_1 & \\ & C_2+(1-\alpha)A_2^T C_0 A_2+(1-\alpha)A_2^T M_0 \dot A_2\end{bmatrix}$$

$$G(q)=\begin{bmatrix} G_1(q_1)+\alpha A_1^T G_0(p)\\ G_2(q_2)+(1-\alpha)A_2^T G_0(p)\end{bmatrix}\qquad D(q)=w)\begin{bmatrix} A_1 & -A_2\\ \alpha J_c(p)A_1 & (1-\alpha)J_c(p)A_2\end{bmatrix}$$

$$\tilde f(q,t)=\begin{bmatrix}\tilde f_1(t)+\alpha A_1^T \tilde f_0(t)\\ \tilde f_2(t)+(1-\alpha)A_2^T\tilde f_0(t)\end{bmatrix}\qquad \tau=[\tau_1^T,\tau_2^T]^T\in R^{n_1+n_2}. \tag{13}$$

By eliminating p, the internal constraints (5) and the external constraints (8) can be written in terms of q as

$$\Phi(q)=0$$

$$\Phi(q)=\begin{bmatrix}\Phi_1(q_1)-\Phi_2(q_2)\\ \alpha\Phi_0(\Phi_1(q_1))+(1-\alpha)\Phi_0(\Phi_2(q_2))\end{bmatrix}\in R^{n_0+m} \tag{14}$$

with property $D(q)=\partial\Phi(q)/\partial q$. Noticing Properties 1–3, (12) has the following properties.

Property 4: $M(q)$ is a symmetric positive definite matrix with $k_q' I_{n_1+n_2}\le M(q)\le k_q'' I_{n_1+n_2}$ where $k_q'=\min[k_1',k_2']$ and $k_q''=\max[k_1'',k_2'']$.

Property 5: The matrix $N(q,\dot q)=\dot M(q)-2C(q,\dot q)$ is a skew-symmetric matrix.

Property 6: A part of the dynamic structure (12) is linear in terms of the selected set $\beta=[\beta_0^T,\beta_1^T,\beta_2^T]^T\in R^{k0+k1+k2}$ with

$$M(q)\ddot q_{eq}+C(q,\dot q)\dot q_{eq}+G(q)=Y(q,\dot q,\dot q_{eq},\ddot q_{eq})\beta \tag{15}$$

where

$$Y(q,\dot q,\dot q_{eq},\ddot q_{eq})=\begin{bmatrix}\alpha A_1^T Y_0(p,\dot p,\dot p_{1eq},\ddot p_{1eq}) & Y_1(q_1,\dot q_1,\dot q_{1eq},\ddot q_{1eq}) & 0\\ (1-\alpha)A_2^T Y_0(p,\dot p,\dot p_{2eq},\ddot p_{2eq}) & 0 & Y_2(q_2,\dot q_2,\dot q_{2eq},\ddot q_{2eq})\end{bmatrix}$$

$$\dot p_{1eq}=A_1\dot q_{1eq}\qquad \ddot p_{1eq}=A_1\ddot q_{1eq}+\dot A_1\dot q_{1eq}\qquad \dot q_{eq}=[\dot q_{1eq}^T,\dot q_{2eq}^T]^T$$

$$\dot p_{2eq}=A_2\dot q_{2eq}\qquad \ddot p_{2eq}=A_2\ddot q_{2eq}+\dot A_2\dot q_{2eq}\qquad \ddot q_{eq}=[\ddot q_{1eq}^T,\ddot q_{2eq}^T]^T. \tag{16}$$

In the constrained robotic system (12), the imposed constraints (14) result in a loss of degrees of freedom of the system which is reduced to $k=n_1+n_2-(n_0+m)$. Therefore, we assume that the robotic system configuration can be characterized by k independent generalized coordinates $\Psi(q)=[\psi_1(q),\cdots,\psi_k(q)]^T$ which are twice continuously differentiable and independent of $\Phi(q)$. In them, (n_0-m) generalized coordinates are used to parameterize the motion of the object on the constraint surfaces. The others are used to characterize the self-movement of the robots when the robots are redundant. When each robot is nonredundant, that is, $n_i=n_0$, $k=n_0-m$, the motion of the robotic system is completely determined by the motion of the object on the constraint surfaces.

The robust motion, internal force, and constrained force control problem of the robotic system is stated as that of designing a controller so that the robotic system with the constraints (14) follows the desired motion trajectory $\Psi(q_d(t))$ while exerting the desired internal force and constrained force $f_d(t)=[f_{intd}^T(t),f_{nd}^T(t)]^T$ under the modeling errors (7).

III. VSC Coordinated Motion and Force Control of Robotic System

Define a nonlinear transformation

$$r(q)=[r_f^T,r_p^T]^T\quad r_f=\Phi(q)\quad r_p=\Psi(q)$$

$$\dot r=J_q\dot q\quad J_q=[D(q)^T,J_{r_p}(q)^T]^T\quad J_{r_p}(q)=\frac{\partial\Psi(q)}{\partial q}. \tag{17}$$

Substituting (17) into (12), multiplying both side by J_q^{-T}, dynamic equation of the robotic system (12) can be expressed in terms of the variable r as

$$H(r)\ddot r+C(r,\dot r)\dot r+G(r)+\tilde F(r,t)=T-Bf$$

$$r=[0,r_p^T]^T\quad B=[I_{n+m},0]^T \tag{18}$$

where

$$H(r)=J_q^{-T}M(q)J_q^{-1}$$

$$C(r,\dot r)=J_q^{-T}C(q,\dot q)J_q^{-1}-J_q^{-T}M(q)J_q^{-1}\dot J_q J_q^{-1}$$

$$G(r)=J_q^{-T}G(q)\qquad \tilde F(r,t)=J_q^{-T}\tilde f(t)\qquad T=J_q^{-T}\tau \tag{19}$$

in which the constraints (14) is simply described by $r_f=0$. The motion of the robotic system is uniquely determined by the coordinates r_p, and the desired motion is given by $r_{pd}(t)=\Psi(q_d(t))$.

From Properties 4–6, (18) has the following properties.

Property 7 [9]: For finite workspace Ω which J_q is nonsingular, $H(r)$ is a symmetric positive definite matrix with $k_r' I_{n_1+n_2}\le H(r)\le k_r'' I_{n_1+n_2}$ where $k_r'=(k_q'/c_1^2)$ $k_r''=(k_q''/c_2^2)$ $c_1=$

$\max_{q \in \Omega}[\sigma_{\max}(J_q(q))]$ $c_2 = \min_{q \in \Omega}[\sigma_{\min}(J_q(q))]$ and $\sigma(J_q)$ means singular value of the matrix J_q.

Property 8 [9]: The matrix $N(r, \dot{r}) = \dot{H}(r) - 2C(r, \dot{r})$ is a skew-symmetric matrix.

Property 9: A part of the dynamic structure (18) is linear in terms of the selected set β in Property 6 with

$$H(r)\ddot{r}_{eq} + C(r, \dot{r})\dot{r}_{eq} + G(r) = Y(r, \dot{r}, \dot{r}_{eq}, \ddot{r}_{eq})\beta \quad (20)$$

where

$$Y(r, \dot{r}, \dot{r}_{eq}, \ddot{r}_{eq}) = J_q^{-T} Y(q, \dot{q}, \dot{q}_{eq}, \ddot{q}_{eq})$$
$$\dot{q}_{eq} = J_q^{-1}\dot{r}_{eq} \qquad \ddot{q}_{eq} = J_q^{-1}(\ddot{r}_{eq} - \dot{J}_q \dot{q}_{eq}). \quad (21)$$

For VSC, the switching function is selected as

$$s = [s_f^T, s_p^T]^T \qquad s_f = K_f \int_0^t e_f(\mu)\, d\mu \qquad e_f = f(t) - f_d(t)$$
$$s_p = \dot{e}_p + K_p e_p \qquad e_p = r_p(t) - r_{pd}(t) \quad (22)$$

where K_f is a weighting matrix, K_p is any positive definite matrix. The resulted sliding mode equation $s = 0$ is described by

$$\int_0^t e_f(\mu)\, d\mu = 0 \qquad \dot{e}_p + K_p e_p = 0 \text{ or } e_p \to 0 \quad (23)$$

and since the integral of e_f vanishes identically for any time t after the sliding mode is reached and maintained, we have, $e_f = 0$, $f = f_d(t)$. The robotic system asymptotically follows the desired motion trajectory $r_{pd}(t)$ while exerting the desired force $f_d(t)$.

The control torque can be determined so that the system reaches the sliding mode in finite time and has prescribed reaching transient response against the modeling errors.

Theorem 1: For the robotic system with the constraints (14), the system will asymptotically follow the desire motion trajectory $r_{pd}(t)$ and exert the desired internal force and external contact force $f_d(t)$ under the modeling errors (7), if the following control torque is applied

$$T = Y(r, \dot{r}, \dot{r}_{eq}, \ddot{r}_{eq})\hat{\beta} - Rs - T_d - \epsilon\, \mathrm{sgn}(s) + Bf \quad (24)$$

where

$$\dot{r}_{eq} = \begin{bmatrix} -K_f \int_0^t e_f(\mu)\, d\mu \\ \dot{r}_{pd}(t) - K_p e_p \end{bmatrix} \qquad \ddot{r}_{eq} = \begin{bmatrix} -K_f e_f \\ \ddot{r}_{pd}(t) - K_p \dot{e}_p \end{bmatrix}$$
$$T_d = [(\delta T)_1 \mathrm{sgn}(s_1), \cdots, (\delta T)_{n_1+n_2} \mathrm{sgn}(s_{n_1+n_2})]^T$$
$$\delta T = |Y(r, \dot{r}, \dot{r}_{eq}, \ddot{r}_{eq})|\delta\beta + |J_q^{-T}|\delta\tilde{f}$$
$$\delta\tilde{f} = \begin{bmatrix} \delta\tilde{f}_1 + \alpha|A_1^T|\delta\tilde{f}_0 \\ \delta\tilde{f}_2 + (1-\alpha)|A_2^T|\delta\tilde{f}_0 \end{bmatrix} \quad (25)$$
$$\epsilon > 0 \qquad \mathrm{sgn}(s) = [\mathrm{sgn}(s_1), \cdots, \mathrm{sgn}(s_{n_1+n_2})]^T$$

R is any positive definite matrix, and $\mathrm{sgn}(\cdot)$ is the sign function. Moreover, the reaching time t_r which the system reaches the sliding mode is

$$t_r \le t_{\max} \qquad t_{\max} = \frac{2}{c_3}\ln\left(1 + \frac{c_3}{c_4}\sqrt{V_0}\right) \quad (26)$$

where

$$c_3 = \frac{2\lambda_{\min}(R)}{k_r''} \qquad c_4 = \epsilon\sqrt{\frac{2}{k_r''}}$$
$$V_0 = \frac{1}{2}s(0)^T H(r(0)) s(0) \quad (27)$$

and the reaching transient response is shaped by

$$\|s\| \le \sqrt{\frac{2}{k_r'}}\left[\left(\sqrt{V_0} + \frac{c_4}{c_3}\right)\exp^{-(c_3/2)t} - \frac{c_4}{c_3}\right] \quad (28)$$

where $\lambda_{\min}(R)$ means minimum eigenvalue of the matrix R. ■

Proof: For the constrained robotic system (18), we choose a Lyapunov function $V = 0.5s^T H(r)s$. From Property 7, we have

$$\frac{1}{2}k_r'\|s\|^2 \le V \le \frac{1}{2}k_r''\|s\|^2. \quad (29)$$

Differentiating V with respect to time yields

$$\begin{aligned} \dot{V} &= s^T H\dot{s} + \frac{1}{2}s^T\dot{H}s \\ &= s^T H\left(\begin{bmatrix} 0 \\ \ddot{r}_p \end{bmatrix} - \ddot{r}_{eq}\right) + s^T C(r, \dot{r})\left(\begin{bmatrix} 0 \\ \dot{r}_p \end{bmatrix} - \dot{r}_{eq}\right) \\ &= s^T[T - H\ddot{r}_{eq} - C(r, \dot{r})\dot{r}_{eq} - G(r) - \tilde{F}(r, t) - Bf] \\ &= s^T[T - Y(r, \dot{r}, \dot{r}_{eq}, \ddot{r}_{eq})\beta - \tilde{F}(r, t) - Bf] \end{aligned} \quad (30)$$

where Property 8 has been used to eliminate the term $1/2s^T\dot{H}s$ due to the time nature of inertia matrix, and Property 9 has been used to simplify the formula. Substituting control torque (24) into it and noticing (29), we have

$$\begin{aligned} \dot{V} &= -s^T Rs - \epsilon s^T \mathrm{sgn}(s) - s^T T_d \\ &\quad - s^T[Y(r, \dot{r}, \dot{r}_{eq}, \ddot{r}_{eq})\Delta\beta + J_q^{-T}\tilde{f}(t)] \\ &\le -s^T Rs - \epsilon s^T \mathrm{sgn}(s) - s^T T_d + |s^T|\,\delta T \\ &\le -s^T Rs - \epsilon \sum_{i=1}^{N_1+N_2} |s_i| \le -\lambda_{\min}(R)\|s\|^2 - \epsilon\|s\| \\ &\le -c_3 V - c_4\sqrt{V}. \end{aligned} \quad (31)$$

So

$$\sqrt{V} \le \left(\sqrt{V_0} + \frac{c_4}{c_3}\right)\exp^{-(c_3/2)t} - \frac{c_4}{c_3} \quad (32)$$

which means that in finite time $V = 0$, i.e., $s = 0$. Moreover, from (29), the reaching transient response is shaped by (28). The upper limit $t_{\max}$ of the reaching time t_r is solved by setting the right hand of (32) equal to zero which is given by (26). ■

Remark 1: In the above theorem, the role of the discontinuous control torque T_d is to overcome the modeling errors (7) so that the system reaches the sliding mode in finite time. Introducing the discontinuous term $\epsilon\, \mathrm{sgn}(s)$ which enhances this effect and enables us to explicitly control the reaching transient. As can be seen from (26), the larger ϵ and $\lambda_{\min}(R)$ are, the smaller $t_{\max}$ will be, i.e., the reaching transient will be shorter. However, if ϵ is large, there would probably appear a strong chattering in practice due to its discontinuity. A better choice is to take small ϵ and large $\lambda_{\min}(R)$, such that the reaching transient is rapid enough and at the same time the chattering is relatively small.

The corresponding control torque in the joint space is given by

$$\tau = Y(q, \dot{q}, \dot{q}_{eq}, \ddot{q}_{eq})\hat{\beta} - J_q^T[Rs + \epsilon \operatorname{sgn}(s) + T_d - Bf] \quad (33)$$

where $\ddot{q}_{eq}, \dot{q}_{eq}$ is defined in (21). In practice the implementation of the control torque (33) results in control chattering since the control law is discontinuous across a sliding surface. Chattering is undesirable because it involves high control activity and may excite the neglected high-frequency dynamics. Moreover, in the case studied, control chattering also cause force response discontinuous since the applied control torque can directly influence the resulted constrained force and internal force, which severely degrades the system performance. For overcoming this problem, the concept of the boundary layer [14] is used, that is, $\operatorname{sgn}(s_i)$ is replaced by the saturation function sat (s_i/Δ_i) where Δ_i is the boundary layer thickness. This leads to the system response within a guaranteed precision as demonstrated in the simulation.

IV. Simulation

Fig. 1 shows two three-DOF planer robots grasping a common object moving on a circular surface. For simplicity, the object is assumed to be point contact with the surface with physical size neglected. The configuration of each robot is shown in Fig. 2. Elements of the matrices in the dynamic equation (1) are given by

$$\begin{aligned}
M_{i11} &= \beta_{i1} + 2\beta_{i5}L_{i1}C_2^i + 2\beta_{i6}(L_{i1}C_{23}^i + L_{i2}C_3^i)\\
M_{i22} &= \beta_{i2} + 2\beta_{i6}L_{i2}C_3^i \qquad M_{i33} = \beta_{i3}\\
M_{i12} &= \beta_{i2} + \beta_{i5}L_{i1}C_2^i + \beta_{i6}(L_{i1}C_{23}^i + 2L_{i2}C_3^i)\\
M_{i13} &= \beta_{i3} + \beta_{i6}(L_{i1}C_{23}^i + L_{i2}C_3^i)\\
M_{i23} &= \beta_{i3} + \beta_{i6}L_{i2}C_3^i \qquad M_{ijk} = M_{ikj}\\
C_{i11} &= -\beta_{i5}L_{i1}\dot{q}_{i2}S_2^i - \beta_{i6}(L_{i1}S_{23}^i(\dot{q}_{i2} + \dot{q}_{i3}) + L_{i2}\dot{q}_{i3}S_3^i)\\
C_{i12} &= -\beta_{i5}L_{i1}(\dot{q}_{i1} + \dot{q}_{i2})S_2^i\\
&\quad - \beta_{i6}(L_{i1}S_{23}^i(\dot{q}_{i1} + \dot{q}_{i2} + \dot{q}_{i3}) + L_{i2}\dot{q}_{i3}S_3^i) \qquad (34)\\
C_{i13} &= -\beta_{i6}(L_{i1}S_{23}^i + L_{i2}S_3^i)(\dot{q}_{i1} + \dot{q}_{i2} + \dot{q}_{i3})\\
C_{i21} &= \beta_{i5}L_{i1}\dot{q}_{i1}S_2^i + \beta_{i6}\left(L_{i1}S_{23}^i\dot{q}_{i1} - L_{i2}\dot{q}_{i3}S_3^i\right)\\
C_{i22} &= -\beta_{i6}L_{i2}\dot{q}_{i3}S_3^i) \qquad C_{i23} = -\beta_{i6}L_{i2}(\dot{q}_{i1} + \dot{q}_{i2} + \dot{q}_{i3})S_3^i\\
C_{i31} &= \beta_{i6}(L_{i1}S_{23}^i\dot{q}_{i1} + L_{i2}(\dot{q}_{i1} + \dot{q}_{i2})S_3^i)\\
C_{i32} &= \beta_{i6}L_{i2}(\dot{q}_{i1} + \dot{q}_{i2})S_3^i \qquad C_{i33} = 0\\
G_{i1} &= (\beta_{i4}C_1^i + \beta_{i5}C_{12}^i + \beta_{i6}C_{123}^i)g\\
G_{i2} &= (\beta_{i5}C_{12}^i + \beta_{i6}C_{123}^i)g \qquad G_{13} = \beta_{i6}C_{123}^i g
\end{aligned}$$

and $F_{ei} = [f_{eix}, f_{eiy}, m_{eiz}]^T$, $C_1^i = \cos(q_{i1})$, $C_2^i = \cos(q_{i2})$, $C_3^i = \cos(q_{i3})$, $S_1^i = \sin(q_{i1})$, $S_2^i = \sin(q_{i2})$, $S_3^i = \sin(q_{i3})$, $C_{12}^i = \cos(q_{i1} + q_{i2})$, $C_{23}^i = \cos(q_{i2} + q_{i3})$, $C_{123}^i = \cos(q_{i1} + q_{i2} + q_{i3})$, $S_{12}^i = \sin(q_{i1} + q_{i2})$, $S_{23}^i = \sin(q_{i2} + q_{i3})$, $S_{123}^i = \sin(q_{i1} + q_{i2} + q_{i3})$. External disturbances are assumed to be $\tilde{f}_i(t) = [5 \sin(0.5\pi t), 5 \sin(0.5\pi t), 0.5 \sin(0.5\pi t)]^T$. $\beta_i = [\beta_{i1}, \beta_{i2}, \beta_{i3}, \beta_{i4}, \beta_{i5}, \beta_{i6}]^T$ is the suitably selected set of the ith robot physical parameters:

$$\begin{aligned}
\beta_{i1} &= I_{i1} + I_{i2} + I_{i3} + m_{i1}l_{ic1}^2 + m_{i2}l_{ic2}^2\\
&\quad + m_{i3}l_{ic3}^2 + m_{i2}L_{i1}^2 + m_{i3}(L_{i1}^2 + L_{i2}^2)\\
\beta_{i2} &= I_{i2} + I_{i3} + m_{i2}l_{ic2}^2 + m_{i3}l_{ic3}^2 + m_{i3}L_{i2}^2\\
\beta_{i3} &= I_{i3} + m_{i3}l_{ic3}^2\\
\beta_{i4} &= m_{i1}l_{ic1} + (m_{i2} + m_{i3})L_{i1} \qquad \beta_{i5} = m_{i2}l_{ic2} + m_{i3}L_{i2}\\
\beta_{i6} &= m_{i3}l_{ic3}. \qquad (35)
\end{aligned}$$

The matrix $Y_i(q_i, \dot{q}_i, \dot{q}_{ieq}, \ddot{q}_{ieq})$ in Property 3 can be directly obtained by substituting (34) into the left hand of (6). Parameter values of the ith robot under study are $m_{i1} = 10$ kg, $m_{i2} = 10$ kg, $m_{i3} = 2$ kg, $I_{i1} = 2$ kgm², $I_{i2} = 2$ kgm², $I_{i3} = 0.5$ kgm², $l_{ic1} = 0.5$ m, $l_{ic2} = 0.5$ m, $l_{ic3} = 0.1$ m, $L_{i1} = 1$ m, $L_{i2} = 1$ m, $L_{i3} = 0.2$ m. Therefore, $\beta_i = [23.52, 7.02, 0.52, 17, 7, 0.2]^T$. The forward kinematic relationship of the ith robot is $x^i = [x_{ei}, y_{ei}, \theta_{ei}]^T = [L_{i1}C_1^i + L_{i2}C_{12}^i + L_{i3}C_{123}^i, L_{i1}S_1^i + L_{i2}S_{12}^i + L_{i3}S_{123}^i, q_{i1} + q_{i2} + q_{i3}]^T$. The dynamic equation of the object is given by

$$\begin{bmatrix} m_0 & & \\ & m_0 & \\ & & I_0 \end{bmatrix}\ddot{p} + \begin{bmatrix} 0 \\ m_0 g \\ 0 \end{bmatrix} + F_c + \tilde{f}_0(t) = \sum_{i=1}^{2} F_i$$

$$p = \begin{bmatrix} x \\ y \\ \theta \end{bmatrix} \quad \tilde{f}_0(t) = \begin{bmatrix} 10 \\ 10 \\ 0.5 \end{bmatrix}\sin\left(\frac{\pi}{2}t\right) \qquad (36)$$

where $F_i = [f_{ix}, f_{iy}, m_{iz}]^T$ are given by (3), and the actual values of m_0, I_0 are $m_0 = 20$ kg, $I_0 = 4$ kgm². Defining $\beta_0 = [m_0, I_0]^T$, from (36), we can obtain the matrix $Y_0(p, \dot{p}, \dot{p}_{eq}, \ddot{p}_{eq})$.

The exact values of the robot parameter β_i and the object parameter β_0 are assumed to be unknown with their estimated values $\hat{\beta}_i = [14, 4, 0.3, 10, 4, 0.1]^T$, $\hat{\beta}_0 = [10, 2]^T$. So we choose the boundaries of the modeling errors (7) as $\delta\beta_i = [10, 4, 0.3, 7, 3, 0.1]^T$, $\delta\beta_0 = [10, 2]^T$, $\delta\tilde{f}_i = [5, 5, 0.5]^T$, $\delta\tilde{f}_0 = [10, 10, 0.5]^T$. The kinematic relationships (4) among the object and the robots are given by $p = [x_{e1} - d_1, y_{e1}, \theta_{e1}]^T = [d_2 - x_{e2}, y_{e2}, -\theta_{e2}]^T$ where $d_1 = 1$ m, $d_2 = 1$ m. The internal constraints (5) are then calculated, and the internal force is defined by (10) where α is chosen as $\alpha = 0.5$. The environmental constraint (8) and the constrained force (9) are given by

$$\sqrt{x^2 + y^2} - d_3 = 0 \quad d_3 = 0.7\,m \qquad F_c = [\cos\varphi \ \sin\varphi \ 0]^T f_n. \qquad (37)$$

As each robot is nonredundant, the motion of the robotic system is determined by the motion of the object on the circular surface. Therefore, we choose generalized coordinates r_p as $r_p = [x, \theta]^T$. The nonlinear transformation (17) are then formed. The switching function is defined in (22) where $K_f = \operatorname{diag}\{0.02, 0.02, 0.02, 0.02\}$ and $K_p = \operatorname{diag}\{15, 15\}$. The control torque is calculated by (33) where $\operatorname{sgn}(s)$ is replaced by sat (s/Δ). The controller parameters are chosen as $R = \operatorname{diag}\{2000, 2000, 2000, 2000, 1000, 1000\}$, $\epsilon = 1$, $\Delta = \operatorname{diag}\{0.03, 0.03, 0.03, 0.05, 0.05, 0.03\}$, $g = 9.8$ ms^{-2}. The desired position, internal force and contact force trajectories are

$$\begin{aligned}
x_d &= -0.5\cos(0.25\pi t)\\
\theta_d &= \operatorname{atan} 2\left[\sqrt{d_3^2 - x_d^2(t)}, x_d(t)\right] - 0.5\pi\\
f_{int} &= [0 \ 0 \ 0]^T \qquad f_n = -50 - 25\sin(0.5\pi t). \qquad (38)
\end{aligned}$$

Figs. 3–5 show the time responses of position, internal force,

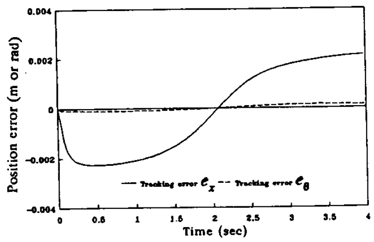

Fig. 3. Tracking error of position of the object.

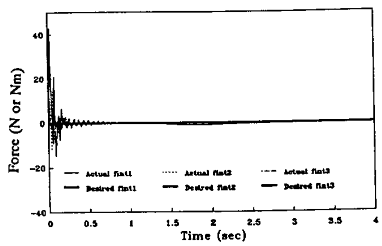

Fig. 4. Time response of internal force f_{int}.

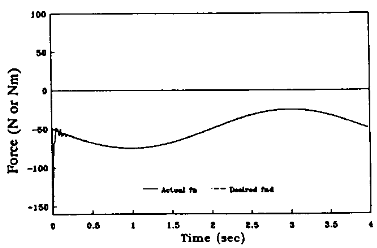

Fig. 5. Time response of contact force f_n.

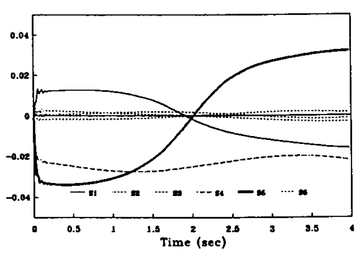

Fig. 6. Time response of switching function.

and contact force of the object which verify the robust motion and force tracking control of the suggested method. The time response of the switching function is shown in Fig. 6. Robot joint torques of Figs. 7 and 8 demonstrate the elimination of chattering by using the boundary layer technique.

V. Conclusion

In this note, the robust motion, internal force, and contact force control problem of two manipulators grasping a common object which interacts with the environment has been considered. Kinematic and dynamic constraints imposed on the manip-

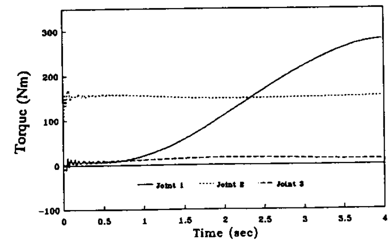

Fig. 7. Joint torque of the robot 1.

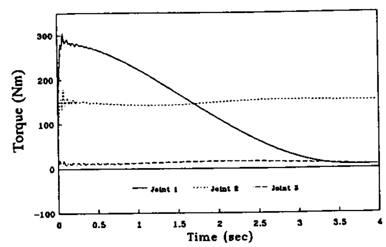

Fig. 8. Joint torque of the robot 2.

ulators and the object are first determined to obtain a dynamic model of the entire system in the joint space. Based on a transformed dynamic equation, motion and force tracking control are designed via a VSC method with robustness to both parametric uncertainties and external disturbances. Prescribed qualities are also guaranteed during the reaching transient. Detailed simulation results illustrate the proposed method.

References

[1] K. Kreutz and A. Lokshin, "Load balancing and closed chain multiple arm control," in *Proc. Amer. Contr. Conf.*, 1988, pp. 2148–2155.

[2] M. Uchiyama and P. Dauchez, "A symmetric hybrid position and force control system for the coordination of two robots," in *Proc. IEEE Int. Conf. Robot. Automat.*, 1988, pp. 350–357.

[3] Xiao Ping Yun, T. J. Tarn, and A. K. Bejczy, "Dynamic coordinated control of two robot manipulators," in *Proc. 28th IEEE Conf., Decision Contr.* 1989, pp. 2476–2481.

[4] J. T. Wen and K. Kreutz, "Motion and force control for multiple cooperative manipulators," in *Proc. IEEE Int. Conf. Robot. Automat.*, 1989.

[5] M. A. Unserem and A. J. Koivo, "Reduced-order model and decoupled control architecture for two manipulators holding an object," in *Proc. IEEE Int. Conf. Robotics Automat.*, 1989, pp. 1240–1245.

[6] M. W. Walker, D. Kim, and J. Dionise, "Adaptive coordinated motion control of two manipulator arms," in *Proc. IEEE Int. Conf. Robot. Automat.*, 1989, pp. 1084–1090.

[7] Xiao Ping Yun, "Nonlinear feedback control of two manipulators in presence of environment constraints," in *Proc. IEEE Int. Conf. Robot. Automat.*, 1989, pp. 1252–1257.

[8] T. Yoshikawa and Xinzhi Zheng, "Coordinated dynamic hybrid position and force control for multiple robot manipulators handling one constrained object," in *Proc. IEEE Int. Conf. Robot. Automat.*, 1990, pp. 1178–1183.

[9] B. Yao, W. B. Gao, and S. P. Chan, "Robust constrained motion control of multiarm robots holding a common object," in *Proc. IEEE Conf. IECON'90*, CA, 1990, pp. 232–237.

[10] Yan Ru Hu and A. A. Goldenberg, "An adaptive approach to motion and force control of multiple coordinated robot arms," in *Proc. IEEE Int. Conf. Robot. Automat.*, 1989, pp. 1091–1096.

[11] N. H. McClamroch and Dan Wei Wang, "Feedback stabilization and tracking of constrained robots," *IEEE Trans. Automat. Contr.*, vol. 33, no. 5, 1988.

[12] J. K. Mills and A. A. Goldenberg, "Force and position control of manipulators during constrained motion tasks," *IEEE Trans. Robot. and Automat.*, vol. 5, no. 1, 1989.
[13] R. Carelli and R. Kelly, "Adaptive control of constrained robots modeled by singular system," in *Proc. 28th Conf. Decision Contr.*, 1989, pp. 2635–2640.
[14] J. J. Slotine, "The robust control of robot manipulators," *Int. J. Robot. Res.*, vol. 4, pp. 49–63, 1985.
[15] S. P. Chan and W. B. Gao, "Variable structure model reaching control strategy for robot manipulators," in *Proc. IEEE Int. Conf. Robot. Automat.*, 1989.
[16] W. B. Gao, "Synthesis of nonlinear control system via variable structure systems," China-Japan Joint Symp. Syst. Contr. Theory Its Appl., Hangzhou, Jan. 25–29, 1989, pp. 103–107.

Discrete-Time Point Process Filter for Mode Estimation

Chun Yang, Yaakov Bar-Shalom, and Ching-Fang Lin

***Abstract*—The performance of a tracking and prediction system of maneuvering targets can be improved by using additional (and unconventional) measurements of target features or attitude (target modes), typically provided by an image sensor processor. A model for the image-based observation channel for target-mode estimation in discrete time is presented in this note. A multidimensional point-process filter is then obtained by using the discrete-time point process theory. The characteristics of the filter are finally illustrated through simulation examples.**

I. Introduction

Maneuver estimation is a major problem in advanced target tracking. The difficulty lies in the uncertainty of the maneuver. Maneuvers can be modeled as acceleration changes in the kinematic equations, and a survey of recent results in the literature can be found in [1]. However, those approaches suffer, as pointed out in [2], from a fundamental limitation when only position (range and angles) and, occasionally, Doppler rate are available. There is a significant delay between the time of an acceleration change and the time when the trajectory deviation permits us to determine that change unambiguously. Consequently, it is difficult to obtain a satisfactory maneuver detection and acceleration estimation only from those measurements.

Introducing a new source of information was proposed in [2], to exploit the significant correlation between the aircraft orientation and the direction of the acceleration. A relationship between aircraft attitude angles (yaw, pitch, and roll) and the magnitude and direction of acceleration was analytically derived in [3]. The use of an imaging sensor, in conjunction with an image processor, provides the practical means to obtain attitude measurements. Most parameters characterizing the target attitude are inherently continuous valued, like orientation angles. However, the precision limitation of processing algorithms and the time constraint involved necessitate attitude variable discretization. The mechanism of optical-matched filters or correlators [4] as well as neural network technology [5] only considers a finite set of reference patterns. These image-processing algorithms express a continuous-valued attitude in terms of a finite set of values or modes, and their output (image-based mode measurement) can be considered as a sequence of statements from a finite vocabulary describing the image content.

Manuscript received February 27, 1990; revised March 20, 1991. The work of C. Yang and Y. Bar-Shalom was supported by The Office of Naval Research under Grant N00014-91-J-1950.
C. Yang and C.-F. Lin are with the American GNC Corporation, Chatsworth, CA 91311-6110. C. Yang completed this work while at the University of Connecticut, Storrs, CT, 06369-3157

Y. Bar-Shalom is with the Department of Electrical and Systems Engineering, University of Connecticut, Storrs, CT 06369-3157.
IEEE Log Number 9203068.

Due to clutter and processing error, the statement from the image sensor processor may not correspond to the actual mode of the target. Temporal filtering is necessary to yield more reliable assessments. A continuous-time probabilistic framework has been established [6] and a mode filter developed to account for the imperfection of image-based mode measurements.

In this note, the discrete-time counterpart is defined, and the discrete nature of image processing is accounted for fully: not only the discrete-valued outputs but also the fact that the output is available only at discrete times. The dependence of image sensing and processing upon the target mode is also taken into account.

II. Discrete-Time Imaging Channel and Mode Filter

Target maneuvering is often slowly reflected in position measurements; whereas the maneuver-induced target orientation change can be quickly detected through the sudden variation of the target image [2], [3], and [6]. The imaging sensor and image processor constitute an image-based observation channel. Assume that the image sensor processor is designed to look from cluttered and noisy images for a set of modes (discretized attitude) of the target of interest, denoted by

$$m(t) \in M = \{1, \cdots, M\}. \tag{2.1}$$

Introduce an indicator vector $\phi(t)$ for $m(t)$ such that the ith element of $\phi(t)$ is

$$\phi_i(t) = \begin{cases} 1 & m(t) = i \\ 0 & \text{otherwise.} \end{cases} \tag{2.2}$$

The output of the image sensor processor is one of the M possible statements denoted by

$$n(t) \in M = \{1, \cdots, M\} \tag{2.3}$$

and a similar indicator vector $\rho(t)$ for $n(t)$. Then, $\rho(t)$ is a vector with binary elements or a point-process vector [7].

Two parameters are introduced to describe the image-sensing and image-processing procedure. The first, observation rate, characterizes the dependence of the image frame and mode statement generation upon the complexity of information, sensitivity of the detector, sophistication of processing, availability of CPU, etc. Denote the appearance of a frame of image by a binary variable such that

$$\iota(t) = \begin{cases} 1 & \text{a statement is generated} \\ 0 & \text{no statement is available.} \end{cases} \tag{2.4}$$

Note that $\iota(t) = 0$ implies $\rho_i(t) = 0$ for all i. This is different from the continuous-time definition, where the waiting time between two observations is assumed to be exponentially distributed [6]. Consequently, a mode-dependent rate is introduced

$$\lambda = [\lambda_1, \cdots, \lambda_M]' \tag{2.5}$$

with

$$\lambda_i \equiv P\{\iota(t) = 1 | \phi_i(t) = 1\} = E\{\iota(t) | \phi_i(t) = 1\}. \tag{2.6}$$